

# Spatial Sensitivity of Macaque Inferior Temporal Neurons

HANS OP DE BEECK AND RUFIN VOGELS\*

Laboratorium voor Neuro- en Psychofysiologie, KULeuven, B-3000 Leuven, Belgium

## ABSTRACT

Recent findings in dorsal visual stream areas and computational work raise the question whether neurons at the end station of the ventral visual stream can code for stimulus position. The authors provide the first detailed, quantitative data on the spatial sensitivity of neurons in the anterior part of the inferior temporal cortex (area TE) in awake, fixating monkeys. They observed a large variation in receptive field (RF) size (ranging from 2.8° to 26°). TE neurons differed in their optimal position, with a bias toward the foveal position. Moreover, the RF profiles of most TE neurons could be fitted well with a two-dimensional Gaussian function. Most neurons had only one region of high sensitivity and showed a smooth decline in sensitivity toward more distal positions. In addition, the authors investigated some of the possible determinants of such spatial sensitivity. First, testing with low-pass filtered versions of the stimuli revealed that the general preference for the foveal position and the size of the RFs was not due simply to TE neurons receiving input with a lower spatial resolution at more eccentric positions. The foveal position was still preferred after intense low-pass filtering. Second, although an increase in stimulus size consistently broadened spatial sensitivity profiles, it did not change the qualitative features of these profiles. Moreover, size selectivity of TE neurons was generally position invariant. Overall, the results suggest that TE neurons can code for the position of stimuli in the central region of the visual field. *J. Comp. Neurol.* 426:505–518, 2000. © 2000 Wiley-Liss, Inc.

**Indexing terms:** receptive field; inferior temporal; object recognition

The visual system is frequently conceptualized as consisting of two functionally distinct streams: a ventral stream from area V1 to the inferior temporal cortex (IT) and a dorsal stream from area V1 to the parietal cortex (Felleman and Van Essen, 1991). Initially, the two systems were differentiated in terms of the attributes that they encode, with the dorsal stream involved in the processing of stimulus location and motion and the ventral stream involved in the computation of object attributes (Ungerleider and Mishkin, 1982). Indeed, electrophysiological studies in the macaque showed that IT neurons are strongly selective for object attributes, such as shape, texture, and color (Gross et al., 1972; Schwartz et al., 1983; Desimone et al., 1984; Tanaka et al., 1991), whereas the response of parietal neurons is strongly dependent on stimulus position (Motter et al., 1987; Blatt et al., 1990; Duhamel et al., 1997). Recently, however, Sereno and Maunsell (1998) found that neurons of the lateral intraparietal area can show shape selectivity, even in a passive fixation task that does not require a motor response. This finding is not surprising from the viewpoint that the parietal cortex also codes those shape attributes that can be important for certain tasks of visuomotor integration

(Goodale and Milner, 1992). It raises the question of whether anterior IT neurons [i.e., inferior temporal cortex (area TE) neurons] can code for stimulus position in addition to their well-documented selectivities for shape and color. Computational work points also to the potential importance of position information for object recognition. Some theoretical models of object representation propose that objects could be coded in a part-based, fragmented way instead of holistically (Hummel and Biederman, 1992; Edelman, 1999). In the former coding scheme, position information can support the representation of the relative positions of parts or shape fragments of the same object (see also Missal et al., 1999).

Studies in anesthetized animals reported large TE receptive fields (RF), usually covering the fovea (Gross et al.,

Grant sponsor: Geneeskundige Stichting Koningin Elizabeth; Grant sponsor: Geconarteerde Onderzoeksocctre; Grant number: 95-99/6.

\*Correspondence to: Rufin Vogels, Laboratorium voor Neuro- en Psychofysiologie, KULeuven, Campus Gasthuisberg, Herestraat, B-3000 Leuven, Belgium. E-mail: rufin.vogels@med.kuleuven.ac.be

Received 22 February 2000; Revised 20 June 2000; Accepted 20 June 2000

1972; Desimone and Gross, 1979; Kobatake and Tanaka, 1994). However, those results do not disagree with the possibility of position coding by TE neurons. Indeed, even large RFs can code for position when the responses within the RF are position dependent and when RFs of different neurons do not overlap completely. Also, different TE neurons could have different optimal stimulus positions and even may show more than one locus of high sensitivity ("hot spots") within their RF. To determine how well TE neurons can code for stimulus position, one needs a quantitative measure of their spatial sensitivity profile. Surprisingly, to our knowledge, no such quantitative RF maps of TE neurons have been published either for anesthetized animals or for behaving monkeys. Thus, the primary purpose of the present study was to obtain high-spatial-resolution RF maps of TE neurons in awake, fixating monkeys to assess their spatial sensitivity.

A consistent finding in previous studies is that the response of most TE neurons is larger at the fovea than at more peripheral positions, at least for the few peripheral positions that were tested (Schwartz et al., 1983; Tovee et al., 1994; Ito et al., 1995; Logothetis et al., 1995; Missal et al., 1999). Because spatial resolution decreases with eccentricity at earlier processing stages, as evident from psychophysical experiments in humans and monkeys (Pointer and Hess, 1989; Merigan and Katz, 1990; Levi and Waugh, 1994; García-Pérez and Sierra-Vázquez, 1996; Kiorpes and Kiper, 1996) and neurophysiological data (e.g., in V1; Schiller et al., 1976; Movshon et al., 1978; Van Essen et al., 1984; Tootell et al., 1988), it could be argued that the eccentricity dependence of TE responses is due to a preference for high spatial frequencies. Indeed, the features that are critical to an IT neuron that is selective for subtle shape differences may be present in the high spatial frequencies and, thus, may only be available at small eccentricities. This could explain why some highly selective TE neurons have such small RFs (Logothetis et al., 1995; Missal et al., 1999). Thus, the second purpose of the present study was to determine whether the often observed decrease in response of IT neurons to peripheral stimuli compared with foveal stimuli merely reflects the lower spatial resolution at peripheral positions or, instead, reflects a lower peripheral sensitivity that is relatively independent of spatial frequency. This was tested by measuring the responses of IT neurons to low-pass filtered versions of the original images at foveal and eccentric positions. If the response levels decline peripherally due to a requirement for high spatial frequencies, then one would expect the low-pass filtered versions of the images to produce equally low response levels at foveal positions. Moreover, one would expect that the decline produced by low-pass filtering would be most pronounced for neurons with small RFs.

Third, we studied interactions between the spatial sensitivity of TE neurons and the size of the stimulus that is used to measure this sensitivity. Because the degree of spatial summation could depend on eccentricity, larger stimulus sizes may be needed at peripheral positions compared with foveal positions to obtain similar responses. The latter is not unreasonable given the increase in RF size with eccentricity at earlier stages (e.g., in V1; Van Essen et al., 1984); however, to our knowledge, this has never been studied in the IT. Apart from spatial summation, the responses to stimuli at nearby test regions could become more similar, because stimuli at different test

positions overlap when using larger stimuli, causing an apparent drop in spatial sensitivity. Size could also be important as a stimulus feature, analogous to position and shape. If stimulus size were to be coded in IT, then one would expect that size preferences would be the same at different positions. Thus, whereas other studies focused on invariances in the coding of shape across different sizes and positions (Schwartz et al., 1983; Lueschow et al., 1994; Ito et al., 1995), we also looked for invariance in the coding of size across positions.

## MATERIALS AND METHODS

### Subjects and surgery

Three male rhesus monkeys that had been used in previous experiments (Missal et al., 1999; Vogels, 1999; Vogels et al., 1999) had a search coil implanted in one eye and a stainless-steel head holder cemented to the skull for head fixation. A stainless-steel recording chamber was implanted on the skull, allowing a dorsal approach to anterior IT. All surgical procedures were performed under deep anesthesia (ketamine, 10 mg/kg, i.m.; sodium pentobarbital, 30 mg/kg, i.v.) and aseptic conditions. The refractions of both eyes were measured in each animal and corrected with spherical lenses, if necessary. During the experiment, the monkeys were water-deprived but received dry food ad libitum supplemented with fruit. The procedures followed the National Institutes of Health guidelines for the care and use of laboratory animals.

Two of the three monkeys (monkeys K and J) were killed with an overdose of barbiturate (sodium pentobarbital, 100 mg/kg, i.v.) at the end of the experiment. In the weeks before, several electrode penetrations were made at selected positions using metal electrodes coated with fluorescent dyes. In addition, electrolytic lesions were made containing iron deposits. After perfusion with a solution of formaldehyde (10%) and potassium ferrocyanide (3%; Prussian blue reaction), the brain was cut, and the 60- $\mu$ m sections were examined using a fluorescent microscope. These sections were stained with cresyl violet, and recording positions were reconstructed using the locations of 1) the tracks of reference wires implanted just before perfusion, 2) the fluorescent electrode tracks, 3) microlesions, 4) iron deposits, and 5) the depth readings of the neurons and location with respect to the pattern of gray/white matter transitions as observed during the recordings. The photomicrograph in Figure 3B was digitized and converted to gray scale (but otherwise was not altered) using Adobe Photoshop software (Adobe Systems, Mountain View, CA). Recording sites in the third monkey (monkey A) were estimated using a superposition of preoperative magnetic resonance imaging and postoperative skull computed tomography scan images. The latter were obtained with the guiding tube in situ. These estimates were confirmed histologically.

### Apparatus

The apparatus is similar to that described in our previous studies (see Vogels, 1999). In the present study, a 21-inch display (Phillips, Matawah, NJ) was positioned 41 cm from the monkey's eyes, providing a 51° (horizontal) by 39° (vertical) field. The monkey was seated in a primate chair, and the head was fixed facing the display. Eye position, which was monitored using the scleral search coil

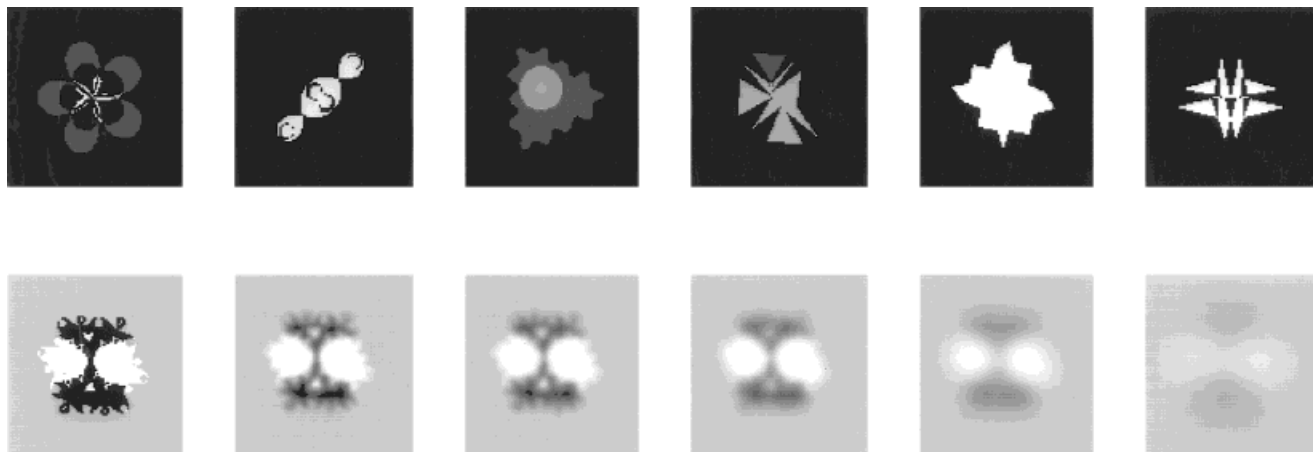


Fig. 1. Illustration of stimuli. Top: Six stimuli from the basic set of 50 stimuli used in monkeys K and J. Bottom: Stimulus from the basic set of 30 stimuli used in monkey A with its five low-pass filtered versions (left, original image; right, most filtered version).

technique, was sampled at 200 Hz. Single-cell recordings were made using tungsten electrodes (kapton and parylene coated: World Precision Instruments [WPI] and Frederick Haer Company [FHC]; impedance, 1–3 M $\Omega$ ) lowered into a guiding tube using a Narishige microdrive, which was securely fixed to the recording chamber. Action potentials of single neurons were isolated on line with a template-matching, spike-sorting system (Real Time Waveform Discriminator; Signal Processing Systems). The spike times and stimuli and the behavioral events were displayed on line and stored for later in-depth analysis. The average number of spikes occurring within a fixed time window (usually 300 msec after stimulus onset) for each stimulus or for each position was updated and displayed continuously during the recordings, allowing on-line selection of optimal stimulus parameters.

### Stimuli

Stimuli were computer-generated Fourier descriptor (FD) shapes created with the algorithm of Zahn and Roskies (1972). Two stimulus sets were used: a set of 50 Fourier shapes in which some component parts were differently colored and 1 of 30 achromatic Fourier shapes and their filtered counterparts. These stimuli were available in four sizes ranging from the standard size of 3.3° to 13.2°. Gray level images of some of these stimuli are shown in Figure 1.

The colored Fourier shapes were presented on a black background with a luminance of 0.03 cd/m<sup>2</sup>. The achromatic Fourier shapes were designed in such a way that their average luminance matched that of the gray background (5.2 cd/m<sup>2</sup>). For each of these 30 shapes, five different low-pass filtered versions were computed with the same average luminance as the unfiltered image and background. The low-pass filtering was performed with two-dimensional, circular Gaussian filters. Each original image was filtered with 5 Gaussians with S.D.s of 0.15, 0.3, 0.59, 0.89, and 1.18 cycles/deg; (Fig. 2), with larger S.D.s corresponding to higher cut-off frequencies. These filters preserve the DC component (mean luminance) and produce no “ringing.” The image contrast (Michelson contrast ratio of 99% for the unfiltered images) decreases with

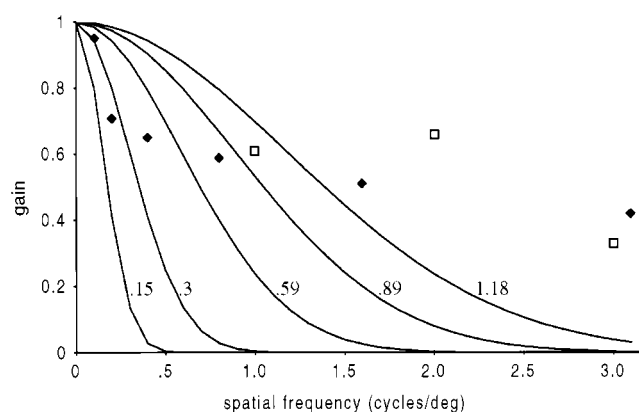


Fig. 2. The five Gaussian filters that were used for the low-pass filtering of the images. The number at each curve refers to the S.D. of the Gaussian. The solid symbols refer to the empirical decrease in contrast sensitivity, as inferred from Pointer and Hess (1989), when stimuli are presented at an eccentricity of 12° instead of being presented at the foveal position. The open symbols show this empirical difference for the low spatial frequencies tested with *Macaca nemestrina* (Kiorpes and Kiper, 1996).

decreasing cut-off frequency (Fig. 1), which is a natural result of the elimination of higher spatial frequencies. However, our original stimuli had sharp luminance edges and no smooth shading effects, so most features of our stimuli remain visible after extensive low-pass filtering (in contrast to filtering of shaded images; see Rolls et al., 1985). We did not match the contrasts of the filtered images to those of the unfiltered images, because we wanted to mimic the elimination of high spatial frequencies, resulting in lower contrasts, which occurs with increased stimulus eccentricity. In Figure 2, we plotted the Gaussian filters together with the changes in contrast sensitivity observed psychophysically in *Macaca nemestrina* (Kiorpes and Kiper, 1996) and in humans (Pointer and Hess, 1989) over a range of 0–12° eccentricity. The decrease in gain obtained with the strongest low-pass

filter is greater than the decrease in contrast sensitivity at 12° eccentricity, the average eccentricity for which we tested the effect of low-pass filtering (see below). The gray levels of the unfiltered and low-pass filtered images were corrected for the display luminance/gray level nonlinearity ( $\gamma$  correction).

### Stimulus presentation and behavioral paradigms

A trial consisted of the presentation of one stimulus and started with the onset of target fixation (0.3° diameter). After 700 msec of fixation, the fixation target was switched off, and the monkey was required to hold his gaze at the same position (fixation window, 1.5°). After a delay of 150–700 msec, depending on the animal, the stimulus was presented for 300 msec, after which the fixation target reappeared for 700 msec. When the monkey had maintained his gaze in the fixation window during the course of the trial, he was rewarded with apple juice. The fixation target was eliminated during stimulus presentation to avoid the possibility that the fixation target could interfere with the stimulus (Richmond and Sato, 1987) and to reduce selective attention effects (see Discussion). When the monkey's gaze moved out of the fixation window, the trial was aborted, and no reward was presented. Only unsorted trials were analyzed.

### Tests

It is not feasible to test each neuron with all stimuli presented at all positions. We therefore choose to search for responsive neurons while presenting the stimuli at their standard size (3.3°) only at the fixation position. Indeed, as stated above, previous studies have shown that most IT neurons respond to stimuli presented foveally. Thus, each neuron was first tested with either the set of 50 colored shapes or the set of 30 achromatic shapes. Responsive neurons were then tested in depth with one or more of the tests described below.

**RF mapping.** The best stimulus for the neuron, i.e. that stimulus of the search stimulus set to which the neuron responded most strongly, was presented at each of 56 positions. These positions formed a regularly spaced, 7 × 8 grid with a center-to-center distance of 4°. The grid consisted of seven rows centered on the fixation position. The contralateral visual field was sampled over a wider range (four columns in addition to the one containing the vertical meridian) than the ipsilateral visual field (three columns). The fixation position corresponded to the display's center. The various positions were tested interleaved and in random order for at least four unsorted trials per position (median, five trials). All neurons were tested with the standard stimulus size of 3.3°. For some neurons, the test was repeated with another stimulus or with the same stimulus but at a larger size.

**Low-pass filtering test.** This test was run only after mapping with the 30 black-and-white shapes. The best stimulus and its five low-pass filtered versions (see above) were presented at both the foveal position and at a more eccentric position (usually 12° contralateral). These 12 conditions were presented interleaved in a random order for at least 10 unsorted trials per condition.

**Size test.** The best stimulus was presented at two positions in four different sizes (3.3°, 6.6°, 9.9°, and 13.2°). The two positions consisted of the one at the fovea and one at which the neuron responded less strongly (as deter-

mined in the previous mapping test). The eight conditions were randomly interleaved for at least ten unsorted trials per condition.

### Data analysis

For each trial, the numbers of spikes were counted within two time windows, one just before stimulus onset (baseline activity) and a second time window starting 50 msec after stimulus onset (stimulus-driven activity). The duration of each time window was 300 msec. All neurons included in this report produced a statistically significant response, as assessed by a split-plot design analysis of variance (ANOVA; Kirk, 1968) comparing baseline and stimulus-driven activity. All neurons that responded in the search test and that were mapped met this statistical response criterion. Further analyses were performed on net responses and consisted of the subtraction of baseline from stimulus-driven activity. These analyses are described below (see Results).

### Analysis of spatial sensitivity profile

To analyze the RFs, the net response at each position of the 7 × 8 grid was expressed as the percentage of the maximal net response of the neuron in this test. Linear interpolation was then used to obtain a contour map of the RF of each neuron. We determined the RF size of each neuron by calculating the square root of the area in the contour map that was at or above 50% of the maximum response. This same response criterion has also been used in recent RF mappings in other areas (Duhamel et al., 1997; Rainer et al., 1998; Anderson and Siegel, 1999; Pasupathy and Connor, 1999).

RF irregularity was quantified as the maximum percentage that a "walker" would have to climb to get from the global maximum to any local maximum in the contour map if they minimize the height to be climbed instead of the overall distance. An RF with no local maxima would have an RF irregularity of zero, whereas the RF irregularity of an RF with one or several local maxima will depend on the depth of the valleys between these local maxima and the global maximum. In the latter cases, we searched for the minimum "climbing height" for each local maximum (i.e., height was minimized for each local maximum). Afterward, we compared these minima of all local maxima, and the RF irregularity was defined by the largest minimum "climbing height." For example, if a particular local maximum could be reached from the global maximum by climbing a minimum of 10% but another one would require 30%, then the RF irregularity would be 30%.

To have a more global measure of the regularity of an RF, we computed the fit between the 56 data points and a two-dimensional Gaussian distribution, as expressed by the formula (Bishop, 1995):

$$G(x,y) = \max R * \exp(-0.5 * \mathbf{M}^T * \mathbf{C} * \mathbf{M})$$

$\max R$  = maximum response of a neuron

$$\mathbf{M} = \begin{pmatrix} x - E(x) \\ y - E(y) \end{pmatrix} \text{ with } E(x) \text{ and } E(y) \text{ the mean of } x \text{ and } y$$

$$\mathbf{C} = \mathbf{COV}^{-1} \text{ (COV is the covariance matrix of } x \text{ and } y \text{).}$$

This function ( $G$ ) is a two-dimensional extension of the standard Gaussian function. Raiguel et al. (1995) generalized the formula to manipulate other aspects of the distribution, like its kurtosis, and expressed the exponential term as a polynomial function. The formula above contains only the zero- and second-order power terms of this polynomial function, resulting in a double-symmetric function with elliptic isocontours. With these restrictions, the exponential term of the generalized Gaussian function is equivalent to the two-dimensional extension of the exponential term in the one-dimensional Gaussian distribution. In both cases, this term contains the squared deviation from the mean [one number in the one-dimensional case and a vector ( $M$ ) in the multidimensional case] divided by the variance (or the covariance matrix in the multidimensional case). Because  $G$  is always positive, negative values in the 56 data points were set to 0. From these 56 values, we calculated for each RF mapping the mean position in the horizontal and vertical direction [ $E(x)$  and  $E(y)$ , corresponding to the coordinates of the RF's center of mass], the position variance in each direction [ $V(x)$  and  $V(y)$ ], and the covariance between both directions [ $COV(x,y)$ ]. A neuron with generally higher responses in the contralateral visual field compared with the ipsilateral visual field will have a mean horizontal position,  $E(x)$ , that is shifted contralaterally. The position variances are an alternative measure of RF size. Using these five parameters, we computed  $G$  at the 56 positions. Finally, we calculated the correlation between these 56 function values and the 56 data points. The square of this correlation ( $R^2$ ) reflects the fit between the function values and the data.  $R^2$  is equivalent to the proportion of variance in the data that can be explained by the model.

Several sources of variance can cause  $R^2$  to be less than 1. We computed the expected decrease in fit that would be induced by measurement noise, i.e., in a case in which the "real" spatial sensitivity profile of a neuron was indeed a Gaussian function, what would be the effect of measuring this profile using a limited number of trials? We started from the 56 function values derived from  $G$  with the parameters set to the appropriate values for each neuron. Gaussian noise was added to these function values, with the variance computed according to the empirically plausible formula:  $\log(\text{variance}) = 1.1 \times \log(\text{mean response}) + 1.5$  (see, e.g., Vogels and Orban, 1995; McAdams and Maunsell, 1999). Because such relation has been found for absolute instead of net responses, the mean response in the above formula corresponds to the function values corrected by adding the mean spontaneous firing rate of each neuron. Furthermore, the S.D.s of these normal distributions were divided by the square root of 5, because most of our RF mappings used five trials at each position. We treated these "noisy," simulated data in the same manner as the real data in computing the appropriate parameter values for the Gaussian function. These parameters can differ slightly from the values found with the actual data, resulting in a new Gaussian function ( $G_n$ ). Finally, we computed the fit ( $R_n^2$ ) between  $G_n$  and the "noisy" data.

## RESULTS

We mapped the RFs of 72 responsive IT neurons (34, 34, and 4 neurons in monkey K, A, and J, respectively). These neurons, as verified by histology, were located in the anterior part of IT (area TE), i.e. in the lower bank of the

superior temporal sulcus and in the cortical convexity lateral to the anterior middle temporal sulcus (Fig. 3).

The 50 colored stimuli were used as the search stimulus set in monkeys K and J, whereas the 30 achromatic, unfiltered FDs were used with monkey A. The RFs of all 72 neurons were investigated, and the most effective stimulus had a size of  $3.3^\circ$ .

### Spatial sensitivity in area TE

RF size, RF position, the regularity of the spatial sensitivity profile, and the consistency of such profiles with different stimuli can determine the capacity of TE neurons to code position.

**Distribution of RF size.** Several contour maps of RFs are displayed in Figure 4. Figure 4A–C shows RFs with a size ranging from  $4.6^\circ$  (Fig. 4A) to  $18.7^\circ$  (Fig. 4C), with Figure 4B displaying an intermediate RF size ( $11.2^\circ$ ). The mean RF of all neurons, calculated after normalizing the responses of each neuron to its maximum response, is shown in Figure 4F. The size of this "population RF" is  $9.6^\circ$ . The distribution of RF size, with a mean of  $10.3^\circ$  and an S.D. of  $5^\circ$ , is shown in Figure 5. Neither the mean maximum response (mean 40.4 spikes per second; ranging from 34.41 spikes per second in monkey A to 46.98 spikes per second in monkey K) nor the mean RF size (ranging from  $9.3^\circ$  in monkey K to  $11.3^\circ$  in monkey A) varied significantly among monkeys; therefore, we pooled the data of the different animals. The smallest RF measured  $2.8^\circ$ , and only two neurons had RFs close to the maximum size ( $25.9^\circ$ ) that is theoretically possible using a grid of  $28^\circ \times 24^\circ$ . It should be noted that the RF size is underestimated for 31 of the 72 neurons, because the 50% contour line for these 31 cells crossed the border of our  $7 \times 8$  grid (see, e.g., Fig. 4C,4E; nonhatched bars in Fig. 5). Sixty-five percent of these 31 neurons responded above 50% at only one (11 neurons) or two (9 neurons) positions at the border of the grid. It is clear that the underestimation will be small for these neurons, at least if we assume that they do not respond strongly at some isolated, peripheral positions outside the grid area (this is unlikely, because we found progressively weaker responses at more peripheral positions; Fig. 4F). The median number of border positions with responses above 50% equaled 6 for the remaining 11 cells (15% of the population). Thus, although the RF size will have been underestimated heavily for some neurons, the underestimation is likely to be small for the large majority of neurons.

The large variation in RF size was found not only across the population of 72 neurons but also within samples of neurons recorded in penetrations with the same anterior-posterior/medial-lateral position. We have a sample of 10 or more neurons at two positions in monkey K and at one position in monkey A. At the first position ( $n = 15$ ), RF size ranged from  $2.8^\circ$  to  $16.1^\circ$  (mean,  $8.4^\circ$ ; S.D.,  $4.5^\circ$ ), at the second position ( $n = 13$ ) from  $3.2^\circ$  to  $18.7^\circ$  (mean,  $10.5^\circ$ ; S.D.,  $4.2^\circ$ ), and at the third position ( $n = 10$ ) from  $3.5^\circ$  to  $19^\circ$  (mean,  $9.2^\circ$ ; S.D.,  $5.3^\circ$ ). The S.D. of the distribution of RF size at one particular penetration was comparable to the S.D. in the whole population. Moreover, we found no significant correlation between anterior-posterior position and RF size [correlation coefficient ( $r$ ) = 0.09;  $n = 34$ ; not significant] in monkey A, in which the penetrations covered a 7-mm range in the anterior-posterior position (the anterior-posterior positions in mon-

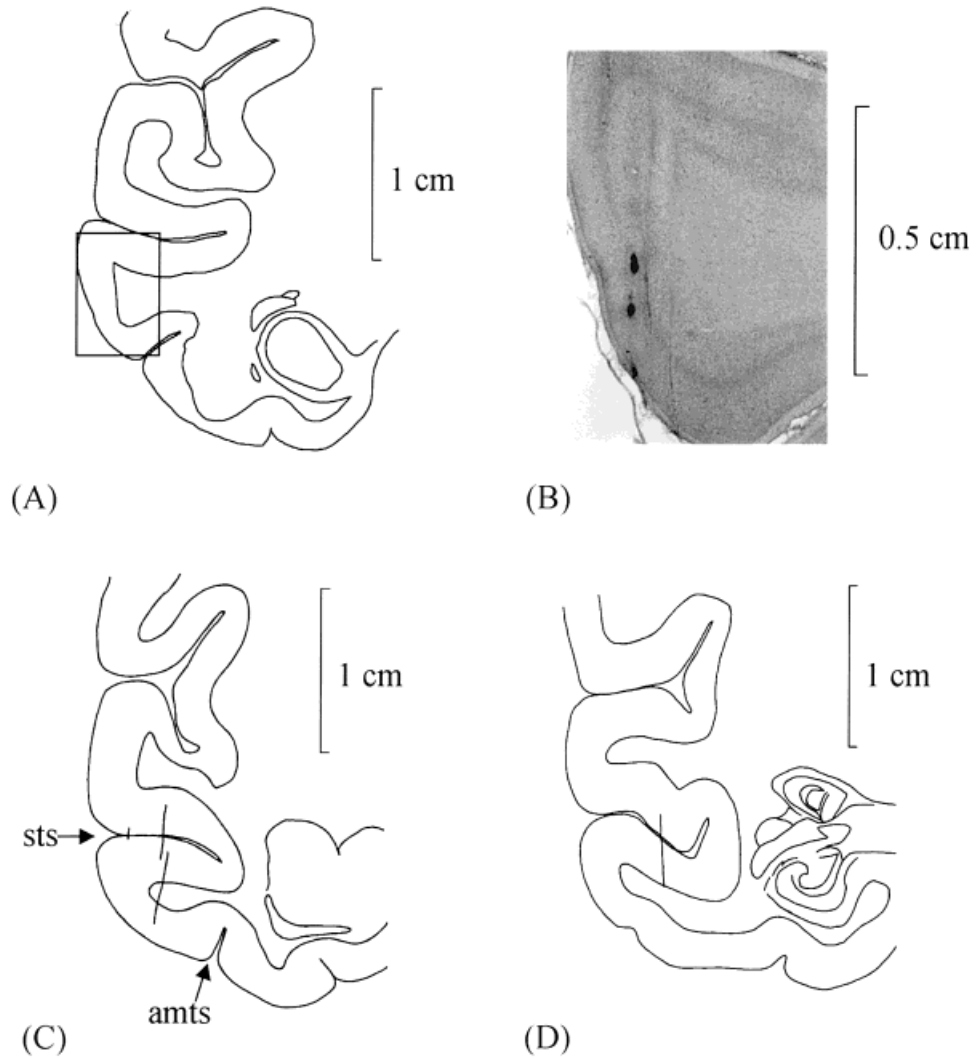


Fig. 3. Recording sites in monkeys K and A. **A:** Line drawing of a coronal section from monkey K in the anterior-posterior range that we recorded from. **B:** Photomicrograph of the outlined part of the coronal section in A showing several electrode tracks and electrolytic lesions

with iron deposits. **C,D:** Line drawings of coronal sections from monkey A at the most anterior (C) and posterior (D) positions we recorded from. amts, Anterior-medial temporal sulcus; sts, superior temporal sulcus.

key K were too clustered to make such an analysis feasible).

**RF position.** Whereas the sizes of RFs varied greatly, many were qualitatively similar to the mean RF shown in Figure 4F, insofar as they had a maximum response rate at the fovea and a gradual decline toward more peripheral positions. To quantify RF position, we used two different measures. First, we computed the center of mass of the RF, including only the positions above 50% of the maximum response and excluding the most contralateral position (to make sure that a bias toward the contralateral hemifield was not a mere consequence of sampling the contralateral visual field more extensively). A plot of these centers of mass (Fig. 6A) shows that these means were distributed over the foveal and parafoveal visual fields. Neurons differed in their optimal positions, but, on the other hand, the optimal position rarely deviated more than  $4^\circ$  from the foveal position. Moreover, there was a

bias toward the contralateral visual field. Such bias is also reflected in a significant difference (Wilcoxon matched-pairs test;  $P < 0.0001$ ) between the contralateral RF size ( $7.7^\circ$ ) and the ipsilateral RF size ( $5.9^\circ$ ).

In a second measure of RF position, we calculated the percentage of neurons that responded above 90% of their maximum responses at a given position. The foveal position lay within the 90% region of the RF for 37 of 72 neurons (51%). For the other neurons (see, e.g., Fig. 4C,E), the optimal position was distributed among the near-peripheral positions again with a bias toward contralateral positions. The probability of finding such a large response in an IT neuron is already very low at only  $8^\circ$  eccentricity. Indeed, very few neurons responded above the 90% criterion at positions outside the central  $3 \times 3$  grid surrounding the foveal position. At 1 position outside this center grid, there were two neurons responding above 90%, at 5 other positions only one neuron reached the crite-

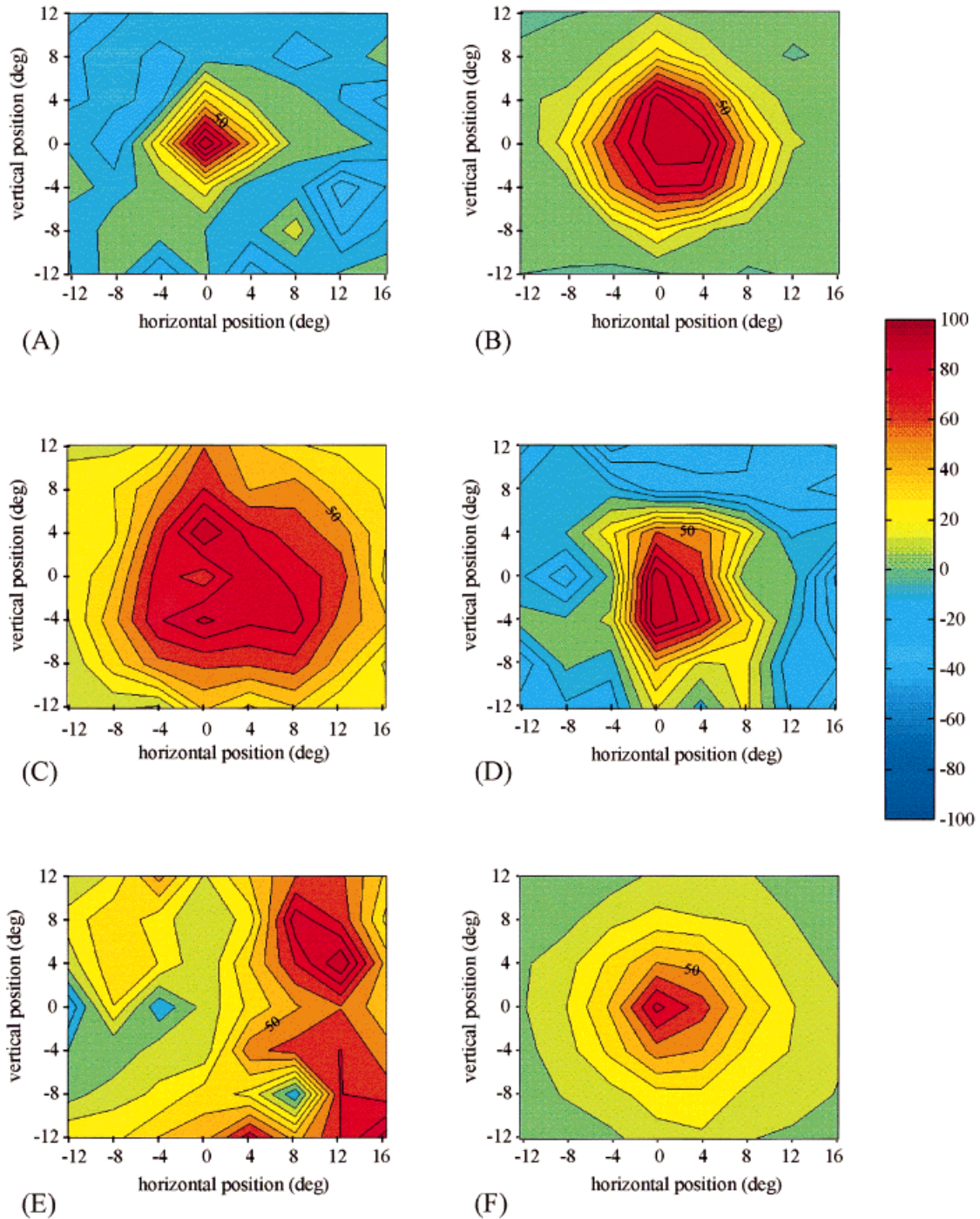


Fig. 4. **A-F:** Contour plots of receptive fields (RF) expressed in percentage of the maximum response. Each line represents a level difference of 10%, and the 50% contour line is labeled. The coordinates (0,0) refer to the foveal position. Negative indices on the vertical and horizontal axes refer to the lower and ipsilateral visual fields, respectively. Plots A-E show RFs from individual neurons with maximum responses of 48, 133, 56, 32, and 41 spikes per second in A-E, respec-

tively. F shows the population RF obtained after normalization of the responses of each neuron to its maximum response. The normalized responses of all neurons were added at each position and then divided by the number of neurons and multiplied by 100. These mean population responses were not normalized to the response at the preferred position, resulting in a maximum at the fovea below 100.

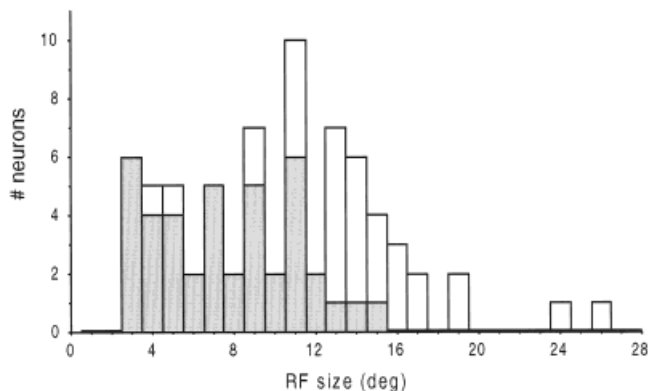


Fig. 5. Distribution of the RF size ( $n = 72$ ). Open bars indicate RFs in which the 50% contour was not completed within the tested visual field area.

tion, and at all 41 of the remaining positions there were no neurons responding above 90% of its maximum response.

Whereas this analysis indicates that the foveal position is preferred to positions at  $4^\circ$  eccentricity by a small majority of TE neurons, it is possible that more subtle differences exist between these “foveal” neurons. We repeated the mapping with a  $7 \times 8$  grid with a resolution of  $1.25^\circ$  instead of  $4^\circ$  for three neurons, two of which preferred the foveal position, and one preferred a contralateral position at  $4^\circ$  eccentricity. One “foveal” neuron still preferred the foveal position, whereas the second actually preferred a position at  $2.5^\circ$  eccentricity in the upper visual field. The third neuron preferred a contralateral position at  $2.8^\circ$ . Thus, our sample of “foveal” neurons will also contain neurons that actually prefer a parafoveal position.

A possible explanation for the general preference for the foveal position is that we searched for responsive neurons with foveal stimulus presentations. Consequently, we recorded only from neurons that seemed to respond foveally and, thus, may have missed neurons with RFs not overlapping the fovea. In monkey A, we attempted to map the RF of neurons not responding to any of the foveal stimuli by presenting each of 30 stimuli at 12 positions covering a similar grid ( $24^\circ \times 16^\circ$ ) but at a lower resolution ( $8^\circ$  between neighboring positions). Each of the 13 neurons formally tested was unresponsive to the stimuli at all tested positions. We were never able to find a neuron that was totally unresponsive at the foveal position while responding at other parts of the visual field. This is not surprising, given the finding that only 2% of visually responsive IT neurons in anesthetized monkeys have an RF that does not include the fovea (Desimone and Gross, 1979). Even if we were to correct our RF properties for this small bias, the general findings would remain unchanged.

Both the large variability in RF size and the variation in RF position are relevant for the capacity of TE neurons to code for stimulus position. With larger RFs, position can only be coded in a distributed manner (Fig. 7A): The response of one such neuron contains only very coarse position information. Nevertheless, by combining the output of neurons with only partially overlapping RFs (Fig. 7A) and graded, position-dependent responses, one can recover stimulus position. The responses of neurons with small RFs (Fig. 7B) convey detailed information about

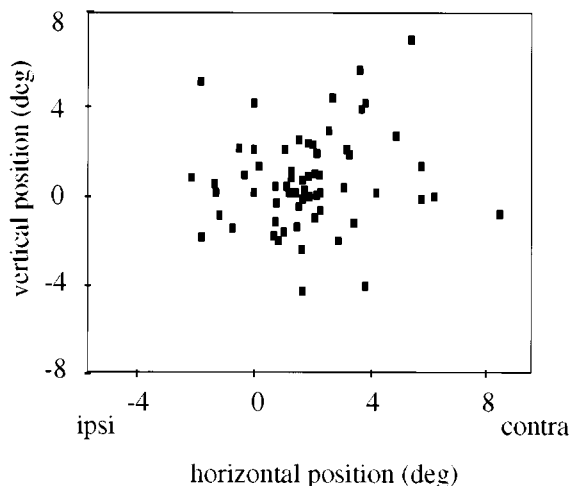


Fig. 6. A scatter plot of the centers of mass of all RFs. The centers of mass were calculated on the responses above 50% of the maximum response, not including the most contralateral (contra) position. Nine RFs had a center of mass exactly at the foveal position. ipsi, Ipsilateral.

where the stimulus was shown. Because we found that optimal position varies between neurons also for those with small RFs (Fig. 7B), these results indicate that TE neurons can provide position information.

**Spatial sensitivity profile of TE neurons.** A third, distinctive property of the RFs is the (ir)regularity of their spatial sensitivity profile. Some RFs were very regular (see, e.g., Fig. 4B), whereas other RF profiles contained several local maxima (see, e.g., Fig. 4E). The RF irregularity (see Materials and Methods) of the different RFs in Figure 4A–E is 20%, 0%, 10%, 0%, and 40%, respectively. Fifty-five neurons (76%) had an RF irregularity less than or equal to 20%. Only three neurons (4%) had RFs that were more irregular than the RF in Figure 4E.

The low measures of RF irregularity suggest that most RFs are very regular and that the appearance of a “hot spot,” excluding the global peak, is not a prevalent feature of the spatial sensitivity profile of TE neurons. However, RF irregularity is a local measure of regularity and can underestimate RF regularity (a high irregularity index can be caused by a single deviant data point). We calculated the fit ( $R^2$ ) between the spatial sensitivity profile of each neuron and a generalized Gaussian function (G), which is a smooth, monotonically decreasing function, as described above (see Materials and Methods). For most neurons, we found a good fit: The mean  $R^2$  was 0.62. Only 18 neurons (25%) had an  $R^2$  value less than 0.50. The  $R^2$  values for the RFs in Figure 4A–E are 0.58, 0.96, 0.82, 0.85, and 0.09, respectively. Figure 8A shows G for the RF of Figure 4C. Several additional sources of variance could contribute to the unexplained 38% of variance in the data. First, the RF profile could be irregular, containing several “hot spots.” Second, the RF profile could be highly regular but possess some characteristics that were not adequately represented in the Gaussian function. For example, we did not manipulate higher order aspects of the function, like skewness and kurtosis. Third, measurement noise could result in an imperfect fit even if the RF profile does have the form of a generalized Gaussian function. We simu-

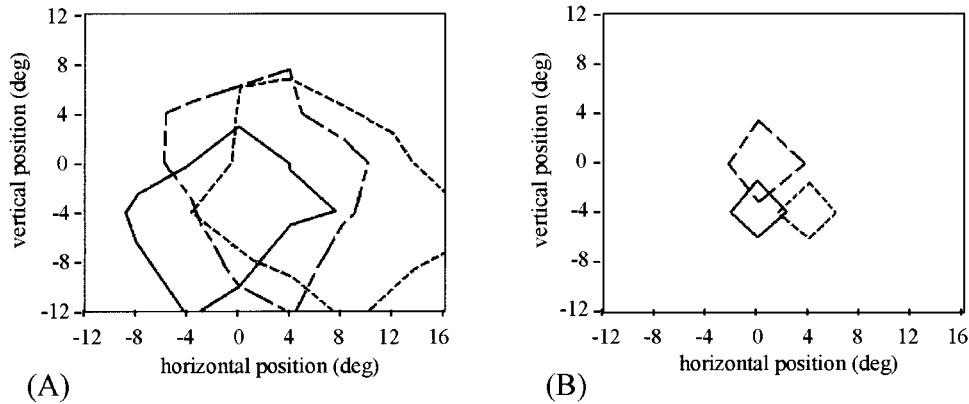


Fig. 7. Fifty-percent contour lines of different RFs plotted on the same scale shown in Figure 4. **A:** Three RFs with a large size (mean size, 13.5°). **B:** Three small RFs (mean size, 3.5°).

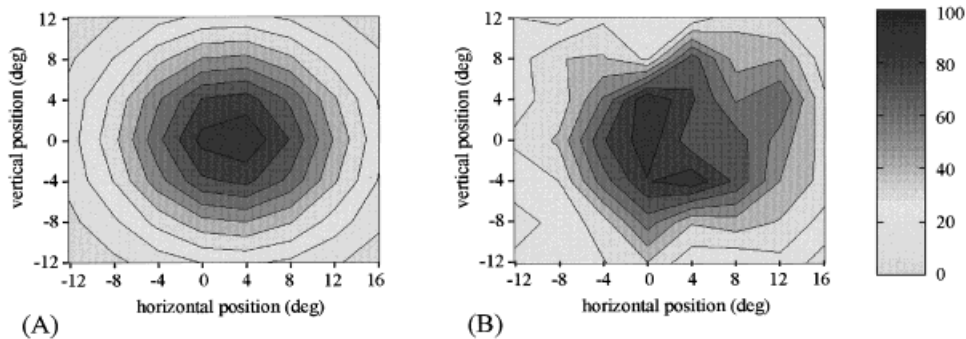


Fig. 8. **A:** An elliptic Gaussian function with the five parameter values adapted to the characteristics of the RF shown in Figure 4C. Like the standard contour plots, all values are expressed as the percentage of the maximum value. **B:** The same Gaussian function after the addition of noise that is proportional to the absolute response.

lated the effect of the latter additional source of variance by putting random fluctuations on the Gaussian function, as described above (see Materials and Methods). Figure 8B shows the same function that was shown in Figure 8A but now with the addition of noise. Across all neurons, the mean  $R^2$  value between these “noisy” data and the Gaussian function (Gn) fitted to these simulated data was 0.74. Because we found a value of 0.62 for the real data (see above), this indicates that, in population terms, only 12% of the variance in the data is due to other factors like skewness, kurtosis, and multiple hot spots. Only limited numbers of neurons had a high RF irregularity, as described above, suggesting that they had more than one distinct region of high spatial sensitivity (see, e.g., Fig. 4E).

**Consistencies of mappings with different stimuli.** It would be difficult to extract position information from the responses of TE neurons if their spatial sensitivity depended on other stimulus features like the color or the shape of the presented stimulus. To investigate this issue, we mapped the RFs of six neurons with two stimuli that elicited comparable responses. The different attributes of these two RF mappings were highly consistent. The correlation between the RF sizes across these six neurons was statistically significant ( $r = 0.84$ ;  $P < 0.05$ ). These

neurons differed greatly in their RF (the ratio of the largest RF to the smallest RF, averaged across the two mappings per neuron, equaled 3.48), but each neuron had similar RF sizes for the two stimuli (mean ratio between RF sizes for the 2 stimuli, 1.22; maximum ratio, 1.37;  $n = 6$ ). Thus, neurons with relatively large RFs, as mapped with one stimulus, also tend to have large RFs for another stimulus. As a measure of position consistency, we computed the mean of each RF mapping in the horizontal and vertical direction. The correlation between the RF positions of the two mappings was again significantly larger than zero in both the horizontal direction ( $r = 0.87$ ;  $P < 0.05$ ) and the vertical direction ( $r = 0.77$ ;  $P < 0.05$ ). The mean within-neuron, absolute deviation in RF position between the two mappings was 0.8° in both directions (maximum, 2°). The maximum between-neuron deviation was 7° in the horizontal direction and 5° in the vertical direction.

### Effect of low-pass filtering

Twenty-nine neurons were tested with the low-pass filtered images. The peripheral position was always contralateral, usually at 12° (22 neurons). Two neurons were tested at 8°, whereas the remaining five neurons were tested with a peripheral position of more than 12°. We

hypothesize above that the general preference of IT neurons for the fovea could reflect a selectivity for higher spatial frequencies. Because only those neurons with a preference for the foveal position are relevant for testing this suggestion, we restricted the analyses described below to the 22 neurons that showed significantly higher responses at the foveal position than at the peripheral position for presentations of the unfiltered stimulus (a priori contrast;  $P < 0.05$ ). An ANOVA for each of these 22 neurons with position and low-pass filtering as factors revealed a significant main effect of position in all neurons. A significant main effect of low-pass filtering was observed in 18 cases (82%). In almost all of these cases ( $n = 17$ ), the response diminished with highly filtered images. Both effects were modulated by a significant interaction in 12 neurons (for examples with and without such interaction, see Fig. 9A,B, respectively), indicating that the main effects are not present consistently. In all 12 of these cases, there was less difference between the responses at the two positions with highly filtered images. Both these main effects and their interaction were significant in an ANOVA (two-way randomized block factorial design; see Kirk, 1968) on the responses of the 22 neurons tested (Fig. 9C). Notwithstanding the statistical significance of the interaction, the mean response to the unfiltered stimulus at the peripheral position was still significantly lower than the mean response to the most strongly low-pass filtered image at the foveal position ( $P < 0.001$ ). Also, the responses at the two positions were still significantly different for the strongest low-pass filter ( $P < 0.00001$ ). This level of low-pass filtering is much higher than that needed to compensate for differences in sensitivity at foveal and peripheral positions across the entire range of spatial frequencies (Fig. 2); thus, these results contradict the idea that the general preference for the foveal position is a mere consequence of the lower sensitivity at the peripheral visual field.

For the same 22 neurons, we calculated the difference (DI) between the foveal response to the unfiltered image and the foveal response to the most filtered image (normalized by dividing this difference by the foveal response to the unfiltered image). The larger the effect of low-pass filtering at the foveal position, the higher the DI. If neurons with smaller RFs require higher spatial frequencies than neurons with larger RFs, then one would predict a negative correlation between DI and RF size. This prediction was not confirmed, because we found no significant correlation between DI and RF size ( $r = 0.30$ ). The lack of correlation between the effect of low-pass filtering and RF size was confirmed by comparing the latter with DIs computed using each of the other four filters.

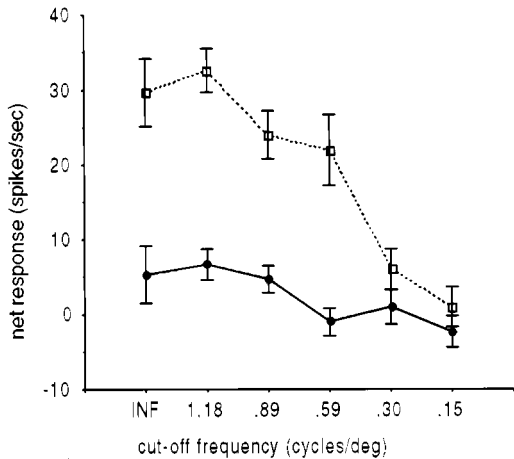
### Effect of stimulus size

The effect of stimulus size on spatial sensitivity profiles was assessed in two ways. First, we replicated the usual RF mapping using the same stimulus but with a larger size in 13 neurons ( $6.6^\circ$  in 11 cases and  $9.9^\circ$  in the other 2 cases). Twelve of the 13 neurons showed a larger RF size when the mapping was performed with a larger stimulus. This effect was significant ( $P < 0.01$ ; Wilcoxon matched-pairs test) and was not associated with an effect of stimulus size on the maximum response to the stimuli ( $P > 0.2$ ). With larger stimuli, the mean RF size increased from  $9^\circ$  to  $12^\circ$ . Notwithstanding the general effect of stimulus size on RF size, there was a significant correlation be-

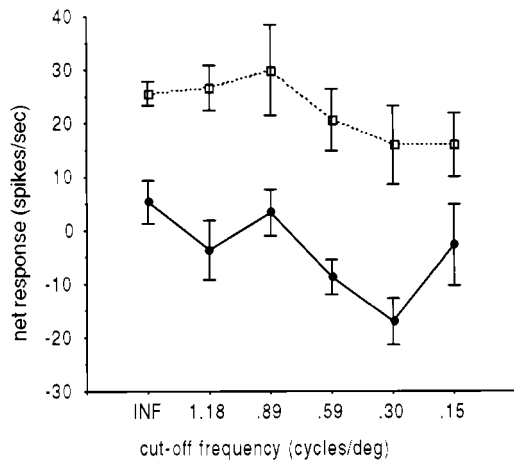
tween the RF size measured with the standard, small stimulus size and the RF size measured with a larger size ( $r = 0.78$ ;  $P < 0.01$ ). Likewise, the centers of mass of both mappings of a neuron were significantly correlated in both the horizontal dimension ( $r = 0.92$ ;  $P < 0.001$ ) and the vertical dimension ( $r = 0.62$ ;  $P < 0.05$ ). The deviations in the mean horizontal position and the mean vertical position between the two mappings were on average  $0.9^\circ$  and  $1.3^\circ$ , respectively (maximum deviation,  $3.9^\circ$ ).

To investigate the effect of stimulus size in more detail, we used the size test described in Materials and Methods for 20 neurons. The peripheral position was always contralateral, usually at  $8^\circ$  or  $12^\circ$  (6 neurons and 12 neurons, respectively; the two exceptions were at  $4^\circ$  and  $13^\circ$ ). For each individual neuron, we performed an ANOVA with position and stimulus size as factors. Sixteen neurons (80%) showed a significant main effect of position. Fifteen of these neurons had a higher response at the foveal position compared with the more peripheral position. Moreover, a significant main effect of stimulus size was found for 15 neurons (75%). Most of these neurons ( $n = 11$ ) showed a higher response with larger stimulus sizes. A significant interaction between position and stimulus size was found in 10 neurons (50%). In six cases, the higher response at the foveal position compared with the peripheral position diminished or reversed with larger stimulus sizes (see Fig. 10A). The four other neurons showed other types of interactions between stimulus position and size (e.g., increase in response with increasing size at the foveal position but not at the peripheral position). A two-way, randomized, block factorial ANOVA on all neurons showed significant main effects of position and size and a significant interaction between the two factors (Fig. 10B). The general pattern is consistent with the results of the mappings with two different stimulus sizes (see above), i.e., 1) the average response shows no effect of size at the foveal position but increases with size at the peripheral position, leading to 2) less difference between responses at foveal and peripheral positions for larger stimulus sizes. These position-dependent effects could be due either to differences in the spatial summation properties between foveal and peripheral positions or to larger stimuli stimulating less peripheral regions than smaller stimuli (e.g., the border of a stimulus of  $13^\circ$  size presented at  $12^\circ$  eccentricity will be at  $5.5^\circ$  eccentricity; the effect of this factor will depend on whether the neuron responds to the border or to a more central feature), or, very likely, to a combination of both of these factors.

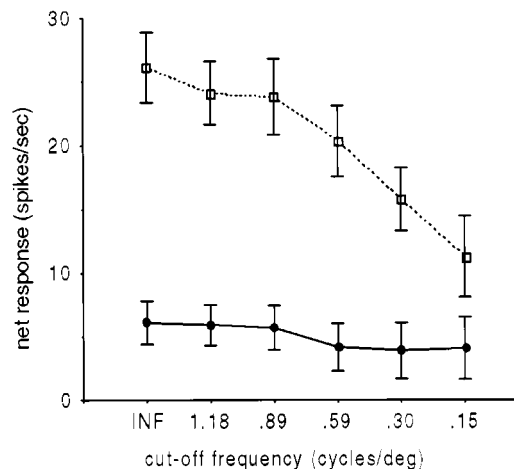
We assessed position invariance of size preference in the same 20 neurons including three additional tests with an ipsilateral position (these tests were not included in the previous group ANOVA to avoid including the foveal responses of some neurons twice). In each of the 23 cases, we ranked the four stimulus sizes according to the response to a given size at the foveal position. If size preferences were to be position invariant, then we would expect to find the same preference at the eccentric position. In a two-way, randomized, block factorial ANOVA on these 23 cases, there was a significant linear trend of size (tested by defining an a priori contrast with orthogonal polynomial coefficients to test linearity; see Kirk, 1968) at the eccentric position [ $F(1,22) = 6.0$ ;  $P < 0.05$ ] with a general preference for the size that was preferred at the foveal position (Fig. 10C). This result indicates that size preferences are generally invariant across positions.



(A)



(B)



(C)

DISCUSSION

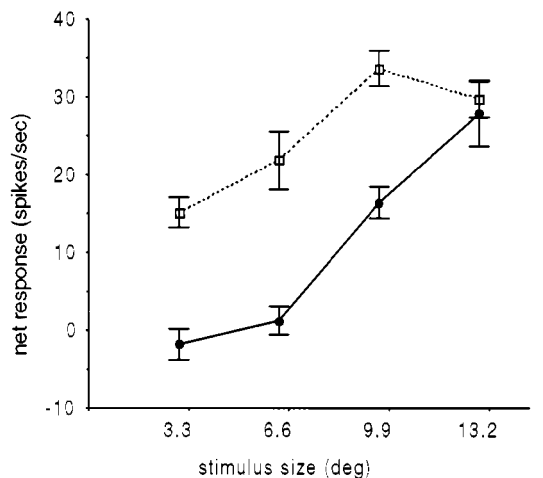
To date, only limited data have been available regarding the spatial sensitivity of TE neurons. One sort of study, performed in anesthetized monkeys, used "hand-plotting" techniques to map RFs (Gross et al., 1972; Desimone et al., 1984; Kobatake and Tanaka, 1994). These studies provided qualitative information regarding spatial sensitivity. Other studies, mainly in awake monkeys, investigated the effect of position quantitatively but examined only a very limited number of positions, usually only along one meridian (Schwartz et al., 1983; Komatsu et al., 1993; Tovee et al., 1994; Logothetis et al., 1995; Missal et al., 1999). All studies agree that TE neurons tend to have larger RFs than neurons in more posterior areas of the ventral visual stream, that they respond most strongly at the foveal position, and that they prefer the contralateral hemifield above the ipsilateral hemifield.

Our results not only confirm and quantify these main properties of RFs in area TE in awake monkeys, but they also provide new information. First, whereas some TE neurons have large RFs, other RFs are surprisingly small. A neuron with a small RF can convey detailed information about position (Fig. 7B), whereas the responses of neurons with large RFs will convey less information without pooling across different neurons (Fig. 7A).

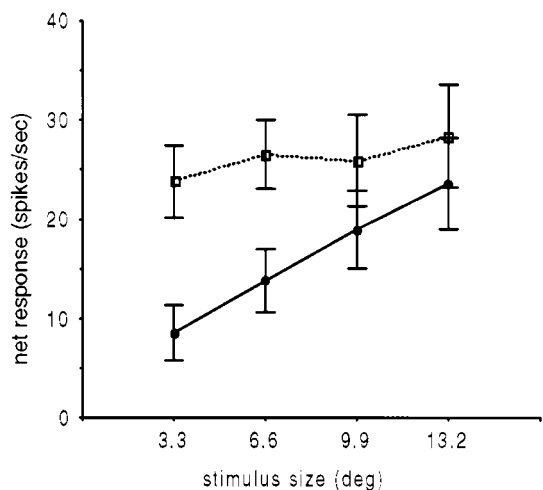
Second, position preferences were distributed in the central visual field. Despite a general trend toward strong responses at the foveal position, almost half of the neurons gave stronger responses to at least one position at 4° eccentricity. Using even more detailed mappings of the parafoveal regions would probably increase the percentage of neurons that prefer nonfoveal positions. Such distribution of position preferences strongly augments the capacity of TE neurons to code for position. However, the finding that the preferred positions were not distributed across the entire visual field but only across the central part suggests that position coding is restricted to this part of the visual field.

Third, the spatial sensitivity profile of TE neurons tends to be very regular. A typical RF profile consists of one global maximum with a gradual fall-off. Consequently, the responses of a neuron to a particular stimulus contain information about how close to the preferred position the stimulus is presented. Such information would be more difficult to extract from the responses of neurons with irregular RFs. Because the maximum responses of half of the neurons were found to be at the foveal position, this general pattern could be partly due to the gradual fall-off in spatial resolution toward more eccentric positions. However, testing with low-pass filtered images revealed that the spatial sensitivity profiles of TE neurons do not

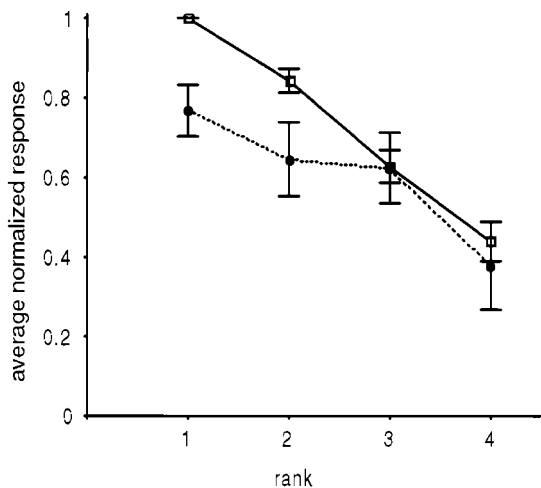
Fig. 9. Examples of the effect of low-pass filtering at the foveal position and at an eccentric position (foveal position, dashed lines and open symbols; eccentric position, solid lines and solid symbols). The filter conditions are ordered in decreasing S.D. of the Gaussian filter with an infinite S.D. (INF) corresponding to the original image. **A:** A typical neuron with an interaction between position and low-pass filtering. The difference between both positions decreases when the images are more filtered. **B:** A neuron without a significant interaction between low-pass filtering and position. **C:** The effect of position and size on the population of neurons that prefer the foveal position (n = 22). Whereas low-pass filtering decreases the difference between both positions, this effect is only partial even with a filter S.D. = 0.15.



(A)



(B)



(C)

reflect their sensitivity in the spatial frequency domain. Moreover, the difference in sensitivity between the foveal position and more eccentric positions is still found after very extensive low-pass filtering. Our finding of a tolerance to low-pass filtering in TE neurons complements that of an earlier study using face stimuli (Rolls et al., 1985) and suggests that the critical shape features driving a TE neuron are not restricted to a particular spatial frequency band.

Fourth, the position sensitivity of TE neurons displayed invariance to shape and size changes. Like what has been found for invariances of shape selectivities (Sáry et al., 1993), the invariance of position sensitivity is not absolute. Indeed, we found that spatial sensitivity decreases with larger stimuli. The main point, however, is that such changes in position sensitivity seem to be quantitative (more or less sensitivity) rather than qualitative (shifts in sensitivity toward a preference for other positions). This is an essential finding, because it makes little sense to draw strong inferences about the spatial sensitivity profile of a neuron if it is found to depend on other factors. Apart from these stimulus properties, spatial sensitivity could also be influenced by task demands, a factor that was not manipulated in the present study. Many studies have found that the responses of neurons throughout the ventral visual pathway are influenced by attentional factors (Richmond et al., 1983; Richmond and Sato, 1987; Desimone and Duncan, 1995; Maunsell, 1995; McAdams and Maunsell, 1999; Reynolds et al., 1999). It should be noted that, in the present study, the fixation spot was absent when the stimulus was flashed, so that the latter was the only stimulus present in the visual field when measuring the neural response.

Attentional effects can be strong when several stimuli are present simultaneously in the visual field or in the receptive field of the neuron, but they are much weaker when only one stimulus is present (Reynolds et al., 1999). Indeed, according to one model of attention (Desimone and Duncan, 1995), the function of selective attention effects is to resolve competition between different stimuli. Apart from avoiding such competition, blinking the fixation target during stimulus presentation may yield the most valid RF estimate. Indeed, Richmond and Sato (1987) compared IT responses to a stimulus when the fixation target was absent with tasks in which the fixation target was present and/or the monkey had to attend the stimulus. The largest responses were obtained in the blinking condition without stimulus attention. Thus, we feel that the RF maps presented here provide a valid measure of the response of IT neurons to single stimuli.

The general invariance of shape preferences when changing other stimulus attributes, such as position, size, and visual cue, suggested that an important function of

Fig. 10. The effect of stimulus size at the foveal position and at an eccentric position (foveal position, dashed lines and open symbols; eccentric position, solid lines and solid symbols). **A:** A typical neuron that responds more to larger stimuli, with this effect most pronounced at the eccentric position (significant interaction). **B:** The effect of position and size on the population of tested neurons ( $n = 20$ ). **C:** The average normalized response (with normalization for each neuron and position separately) plotted as a function of size rank. The sizes were ranked according to each neuron's response strength at the foveal position, and this ranking was applied to both positions.

TE and, more generally, of the ventral visual stream is the representation of the shape of objects, independent of other stimulus attributes (Sáry et al., 1993; Lueschow et al., 1994; Ito et al., 1995). Our results extend this conclusion by showing that TE neurons, at least as a population, also can provide information about shape, position, and size. Of course, our results show only that position information is present, and they are not decisive about whether this information is actually used or, alternatively, whether it is merely a reflection of position sensitivity at earlier processing stages that could not be eliminated completely. However, there is no contradiction between stressing the spatial sensitivity of TE neurons and the idea that the inferotemporal cortex is involved in object identification (Ungerleider and Mishkin, 1982; Logothetis and Sheinberg, 1995). Establishing position and size invariant responses may be one way to construct useful object representations (Wallis and Rolls, 1997). However, it is not necessary to assume that the general position and size invariance in the recognition of objects at the behavioral level is reflected in a position and size invariance of the units that represent these objects. Tanaka and his colleagues (Tanaka et al., 1991; Kobatake and Tanaka, 1994) have shown that most TE neurons prefer shape features that are less complex than most common objects. To decide how these shape features or object "fragments" (Edelman, 1999) are combined into a single, complex shape or which features belong to which object (in cases in which more than one object is present at the time), it would be very helpful to preserve position sensitivity (Edelman, 1999; Missal et al., 1999). Moreover, because primates usually fixate objects of interest, position sensitivity in the central visual field would be more important for object identification compared with position sensitivity in more peripheral positions. Indeed, although our results suggest that TE neurons are not less sensitive for position compared with the spatial sensitivity of parietal neurons (Motter et al., 1987; Blatt et al., 1990; Duhamel et al., 1997), they also indicate that both populations differ greatly with respect to the distribution of RF centers. The RF optima of TE neurons are much less evenly distributed in space: Position coding by TE neurons is more restricted to positions around the fovea.

### ACKNOWLEDGMENTS

The authors thank M. De Paep, P. Kayenbergh, G. Meulemans, A. Coeman, and G. Vanparrys for technical assistance; T. Gautama and M. Van Hulle for advice on image low-pass filtering; M. Van Hulle for suggesting the elliptic Gaussian function; and S. Raiguel for critical reading of an earlier draft of this paper. H.O.d.B is a research assistant and R.V. is a research associate of the Fund for Scientific Research (FWO), Vlaanderen.

### LITERATURE CITED

- Anderson KC, Siegel RM. 1999. Optic flow selectivity in the anterior superior temporal polysensory area, STPa, of the behaving monkey. *J Neurosci* 19:2681–2692.
- Bishop CM. 1995. Neural networks for pattern recognition. Oxford: Clarendon Press.
- Blatt GJ, Andersen RA, Stoner GR. 1990. Visual receptive field organization and cortico-cortical connections of the lateral intraparietal area (area LIP) in the macaque. *J Comp Neurol* 299:421–445.
- Desimone R, Duncan J. 1995. Neural mechanisms of selective visual attention. *Annu Rev Neurosci* 18:193–222.
- Desimone R, Gross CG. 1979. Visual areas in the temporal cortex of the macaque. *Brain Res* 178:363–380.
- Desimone R, Albright TD, Gross CG, Bruce C. 1984. Stimulus-selective properties of inferior temporal neurons in the macaque. *J Neurosci* 4:2051–2062.
- Duhamel JR, Bremmer F, BenHamed S, Graf W. 1997. Spatial invariance of receptive fields in parietal cortex neurons. *Nature* 389:845–848.
- Edelman S. 1999. Representation and recognition in vision. Cambridge, MA: MIT Press.
- Felleman DJ, Van Essen C. 1991. Distributed hierarchical processing in the primate cerebral cortex. *Cereb Cortex* 1:1–47.
- García-Pérez MA, Sierra-Vázquez V. 1996. Do channels shift their tuning towards lower spatial frequencies in the periphery. *Vision Res* 36:3339–3372.
- Goodale MA, Milner AD. 1992. Separate visual pathways for perception and action. *Trends Neurosci* 15:20–25.
- Gross CG, Rocha-Miranda CE, Bender DB. 1972. Visual properties of neurons in inferotemporal cortex of the macaque. *J Neurophysiol* 35:96–111.
- Hummel JE, Biederman I. 1992. Dynamic binding in a neural network for shape recognition. *Psychol Rev* 99:480–517.
- Ito M, Tamura H, Fujita I, Tanaka K. 1995. Size and position invariance of neuronal responses in monkey inferotemporal cortex. *J Neurophysiol* 73:218–226.
- Kiorpes L, Kiper DC. 1996. Development of contrast sensitivity across the visual field in macaque monkeys (*Macaca nemestrina*). *Vision Res* 36:239–247.
- Kirk RE. 1968. Experimental design: procedure for the behavioral sciences. Belmont, CA: Brooks-Cole.
- Kobatake E, Tanaka K. 1994. Neuronal selectivities to complex object features in the ventral visual pathway of the macaque cerebral cortex. *J Neurophysiol* 71:856–867.
- Komatsu H, Ideura Y. 1993. Relationships between color, shape, and pattern selectivities of neurons in the inferior temporal cortex of the monkey. *J Neurophysiol* 70:677–694.
- Levi DM, Waugh SJ. 1994. Spatial scale shifts in peripheral vernier acuity. *Vision Res* 34:2215–2238.
- Logothetis NK, Sheinberg DL. 1995. Visual object recognition. *Annu Rev Neurosci* 19:577–621.
- Logothetis NK, Pauls J, Poggio T. 1995. Shape representation in the inferior temporal cortex of monkeys. *Curr Biol* 5:552–563.
- Lueschow A, Miller EK, Desimone R. 1994. Inferior temporal mechanisms for invariant object recognition. *Cereb Cortex* 4:523–531.
- Maunsell JHR. 1995. The brain's visual world: representations of visual targets in cerebral cortex. *Science* 270:764–769.
- McAdams CJ, Maunsell JHR. 1999. Effects of attention on orientation-tuning functions of single neurons in macaque cortical area V4. *J Neurosci* 19:431–441.
- Merigan WH, Katz LM. 1990. Spatial resolution across the macaque retina. *Vision Res* 30:985–991.
- Missal M, Vogels R, Li CY, Orban GA. 1999. Shape interactions in macaque inferior temporal neurons. *J Neurophysiol* 82:131–142.
- Motter BC, Steinmetz MA, Duffy CJ, Mountcastle VB. 1987. Functional properties of parietal visual neurons: mechanisms of directionality along a single axis. *J Neurosci* 7:154–176.
- Movshon JA, Thompson ID, Tolhurst DJ. 1978. Receptive field organization of complex cells in the cat's striate cortex. *J Physiol* 283:79–99.
- Pasupathy A, Connor CE. 1999. Responses to contour features in macaque area V4. *J Neurophysiol* 82:2490–2502.
- Pointer JS, Hess RF. 1989. The contrast sensitivity gradient across the human visual field with emphasis on the low spatial frequency range. *Vision Res* 29:1133–1151.
- Raiguel S, Van Hulle MM, Xiao DK, Marcar V, Orban GA. 1995. Shape and spatial distribution of receptive fields and antagonistic motion surrounds in the middle temporal area (V5) of the macaque. *Eur J Neurosci* 7:2064–2082.
- Rainer G, Asaad WF, Miller EK. 1998. Memory fields of neurons in the primate prefrontal cortex. *Proc Natl Acad Sci USA* 95:873–877.
- Reynolds JH, Chelazzi L, Desimone R. 1999. Competitive mechanisms

- subserve attention in macaque areas V2 and V4. *J Neurosci* 19:1736–1753.
- Richmond BJ, Sato T. 1987. Enhancement of inferior temporal neurons during visual discrimination. *J Neurophysiol* 58:1292–1306.
- Richmond BJ, Wurtz RH, Sato T. 1983. Visual responses of inferior temporal neurons in awake rhesus monkeys. *J Neurophysiol* 50:1415–1432.
- Rolls ET, Baylis GC, Hasselmo ME. 1985. Role of low and high spatial frequencies in the face-selective responses of neurons in the cortex in the superior temporal sulcus in the monkey. *Vision Res* 25:1021–1035.
- Sáry G, Vogels R, Orban GA. 1993. Cue-invariant shape selectivity of macaque inferior temporal neurons. *Science* 260:995–997.
- Schiller PH, Finlay BL, Volman SF. 1976. Quantitative studies of single-cell properties in monkey striate cortex. III. Spatial frequency. *J Neurophysiol* 39:1334–1351.
- Schwartz EL, Desimone R, Albright TD, Gross CG. 1983. Shape recognition and inferior temporal neurons. *Proc Natl Acad Sci USA* 80:5776–5778.
- Sereno AB, Maunsell JH. 1998. Shape selectivity in primate lateral intraparietal cortex. *Nature* 395:500–503.
- Tanaka K, Saito H, Fukuoka Y, Moriya M. 1991. Coding of visual images of objects in the inferotemporal cortex of the macaque monkey. *J Neurophysiol* 66:170–189.
- Tootell RBH, Silverman MS, Hamilton SL, Switkes E, De Valois RL. 1988. Functional anatomy of macaque striate cortex. V. Spatial frequency. *J Neurosci* 8:1610–1624.
- Tovee MT, Rolls ET, Azzopardi P. 1994. Translation invariance in the responses to faces of single neurons in the temporal visual cortical areas of the alert macaque. *J Neurophysiol* 72:1049–1060.
- Ungerleider LG, Mishkin M. 1982. Two cortical visual systems. In: Ingle DJ, editor. *Analysis of visual behavior*. Cambridge, MA: MIT Press. p 549–586.
- Van Essen DC, Newsome WT, Maunsell JHR. 1984. The visual field representation in striate cortex of the macaque monkey: asymmetries, anisotropies, and individual variability. *Vision Res* 24:429–448.
- Vogels R. 1999. Categorization of complex visual images by rhesus monkeys. Part 2: single-cell study. *Eur J Neurosci* 11:1239–1255.
- Vogels R, Orban GA. 1995. Does practice in orientation discrimination lead to changes in the response properties of macaque inferior temporal neurons. *Eur J Neurosci* 6:1680–1690.
- Vogels R, Biederman I, Bar M. 1999. Sensitivity of macaque inferior temporal neurons to differences in view-invariant versus metric properties of depth-rotated objects. *Invest Ophthalmol Vis Sci* 40:S776.
- Wallis G, Rolls ET. 1997. Invariant face and object recognition in the visual system. *Progr Neurobiol* 51:167–194.
- Zahn CT, Roskies RZ. 1972. Fourier descriptors for plane closed curves. *IEEE Trans Comp* 21:269–281.